

---

---

**STRENGTH  
AND PLASTICITY**

---

---

## **Investigation of the Microstructure and Properties of Al–Si–Mg/SiC Composite Materials Produced by Solidification under Pressure**

**E. A. Mohamed<sup>a, b, \*</sup> and A. Yu. Churyumov<sup>b</sup>**

<sup>a</sup>*Composite Laboratory, Advanced Material Department, Central Metallurgical Research & Development Institute,  
P.O. Box 87 Helwan, 11421 Egypt*

<sup>b</sup>*National University of Science and Technology MISiS, Leninskii pr. 4, Moscow, 119049 Russia*

*\*e-mail: [essam@misis.ru](mailto:essam@misis.ru)*

Received November 3, 2015; in final form, April 5, 2016

**Abstract**—Composite materials based on alloys of the Al–Si–Mg system have been obtained via the introduction of 5, 10, and 15 wt % of SiC particles into the alloy melt and the solidification under a pressure. As a result of solidification under pressure, the porosity of the composite materials decreased substantially. An increase in the content of SiC particles in the composites enabled a smaller size of dendritic cells to be obtained. It has been shown by the X-ray diffraction method that, in the process of solidification under pressure, an interaction occurred between the matrix and reinforcing SiC particles. The presence of SiC particles in the structure of composites led to the acceleration of the aging process and to an increase in the peak hardness in comparison with the matrix alloy.

**Keywords:** metal-matrix composite materials, silicon carbide, microstructure, solidification under pressure, kinetics of aging

**DOI:** 10.1134/S0031918X16100070

### 1. INTRODUCTION

In recent decades, alloys based on light metals have found increasing use in the transport engineering industry because of the significant reduction in their weight and, as consequence, for increasing the energy efficiency of constructions. The ecological aspect of the use of these materials is also of great importance, since aluminum alloys can be reprocessed with relatively low power expenditures. Due to their high casting and mechanical properties, the alloys of the Al–Si–Mg system are the most promising casting alloys [1–3]. However, recently, composite materials based on light metals, such as titanium [4, 5], aluminum [6–9], etc., have also found increasingly wide applications. These materials possess enhanced mechanical properties compared with the usual alloys, e.g., the high modulus of elasticity, high strength and fatigue strength, and high heat resistance and wear resistance. For example, Beffort et al. [2] revealed that the mechanical properties of composites with a metallic matrix and high volume fraction of SiC particles obtained by solidification under pressure are improved significantly because of strengthening due to the presence of ceramic particles and heat treatment. Ranganath et al. [10] and Seah et al. [11] have shown that, with an increase in the content of the reinforcing par-

ticles from 2 to 6 wt %, mechanical characteristics, such as the ultimate strength, yield stress, and hardness, increase substantially, whereas the plasticity and impact toughness are reduced.

Liquid-phase methods of obtaining composite materials are currently among the most widely applicable due to their low cost and high productivity. Among these methods, the process of the mixing of particles into the melt is one of the most economically advantageous and, therefore, widespread methods of the production of composites reinforced by particles [12–15]. Solidification under pressure makes it possible to obtain minimum gas and shrinkage porosity, excellent surface quality, and low material losses. Furthermore, an increase in the rate of cooling in the process of solidification under pressure leads to the formation of finely dispersed structure [16]. Thus, solidification under pressure is one of the most promising methods of obtaining composites in short periods with low expenditures [3, 17].

It is known that the properties of composites with a metallic matrix reinforced by particles depend mainly on the volume fraction and size of particles. The composites with a high volume fraction of particles usually show high porosity and nonuniformity of the particle distribution in the matrix. A uniform particle distribu-

tion in the matrix is necessary to reduce stresses that arise upon loading and, as a consequence, to improve the mechanical properties [18].

## 2. EXPERIMENTAL

As the matrix material, we selected an aluminum Al–9.1Si–0.58Mg alloy. To prepare the alloy, the following commercial materials have been used: aluminum (99.85 wt %), silicon (99.9 wt %), and magnesium (99.9 wt %). The matrix alloy was obtained by melting in a muffle furnace and casting into a graphite mold. To obtain composites, particles of SiC with sizes of 35–45  $\mu\text{m}$  were introduced into the melt (Fig. 1) in amounts of 5, 10, and 15 wt %.

The composites were obtained by mixing particles into the melt and subsequent solidification under pressure using the following technology: 500 g of the matrix alloy were placed into a crucible and heated to a temperature that was 100 K higher than the liquidus temperature of the alloy. After melting, ceramic particles were introduced and mixed using a titanium blade that was rotated at a rate of 850 revolutions per minute for 1 min. After this, the melt was cast into a graphite mold. The process of the solidification under pressure was implemented at a temperature of 620°C using a hydraulic press with a maximum effort of 100 tons. The finished alloy was placed into a cylindrical form with a diameter of 50 mm and a length of 100 mm. After reaching a required temperature, the form with the melt was loaded until a stress of 100 MPa was reached and held under pressure for 1 min, after which the solidified casting was cooled and extracted from the form.

An analysis of the microstructure of samples was carried out using a Bruker D8 Advance diffractometer in a monochromated Cu  $K\alpha$  radiation, a Carl Zeiss Axiovert 200 optical microscope, and a Tescan Vega 3 LMH scanning electron microscope equipped with an X-max 80 energy-dispersive detector. The samples were polished mechanically using a Struers LaboPol-5 grinding-polishing machine.

The density of the samples was determined by the method of hydrostatic weighing on a Vibra AF analytical balance. The theoretical density of the composites was calculated according to the rule of mixture; the densities of the matrix alloy and of the SiC particles were accepted to be  $\rho_{\text{mat}} = 2.67 \text{ g/cm}^3$  and  $\rho_{\text{SiC}} = 3.21 \text{ g/cm}^3$ , respectively [13]. The porosity was calculated via the formula

$$P = \frac{\rho_{\text{theor}} - \rho_{\text{exper}}}{\rho_{\text{exper}}} \times 100\% \quad (1)$$

$$= \left( \frac{V_{\text{SiC}}\rho_{\text{SiC}} + (1 - V_{\text{SiC}})\rho_{\text{mat}}}{\rho_{\text{exper}}} - 1 \right) \times 100\%,$$

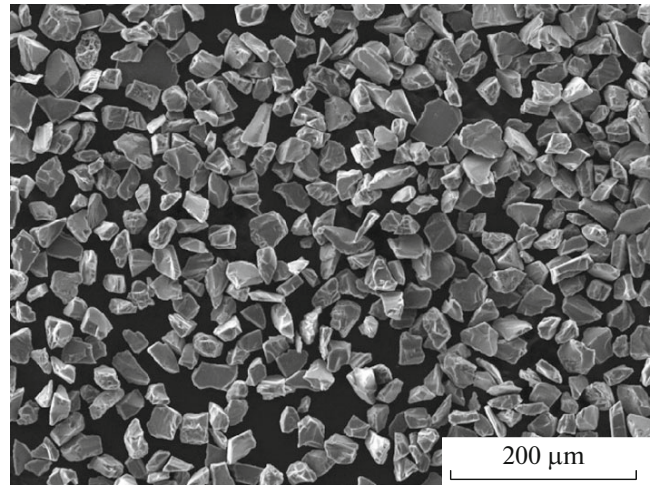


Fig. 1. Microstructure of the initial powder of SiC (SEM).

where  $\rho_{\text{theor}}$  is the theoretical density,  $\text{kg/m}^3$ ;  $\rho_{\text{exper}}$  is the experimental density,  $\text{kg/m}^3$ ; and  $V_{\text{SiC}}$  is the volume fraction of the SiC particles.

The heat treatment of the composites was performed in a Nabertherm furnace in two stages: the first stage is the annealing at 580°C for 8 h and quenching into warm water; the second stage is aging at 155°C with different holding times. After aging, measurements of hardness were performed on an IT5010 hardness meter under a load of 5 kg.

## 3. RESULTS AND DISCUSSION

### 3.1. Density of the Matrix Alloy and Composites

The values of the density of samples with the different contents of SiC in the cast state and after solidification under pressure are given in Fig. 2a. As can be seen, in the process of solidification under a pressure of 100 MPa, the density of both the base alloy and composites on its basis increases. Furthermore, it can be noted that, with an increase in the content of SiC, both the experimental and theoretical density increase because of the higher density of the reinforcing particles ( $3.21 \text{ g/cm}^3$ ) compared with the base alloy. As can be seen from Fig. 2b, as a result of solidification under pressure the porosity of samples is reduced significantly. This is connected with the fact that the pressure acting on the liquid metal before and during solidification leads to a reduction of the amount of gas that was dissolved in the process of the incorporation of the particles. It has been established that the porosity of the composites in the cast state increases with an increase in the content of SiC particles because of the larger amount of incorporated gases; therefore, the use of the second technological process, solidification under pressure, is especially necessary for obtaining composites with a small volume fraction of voids.

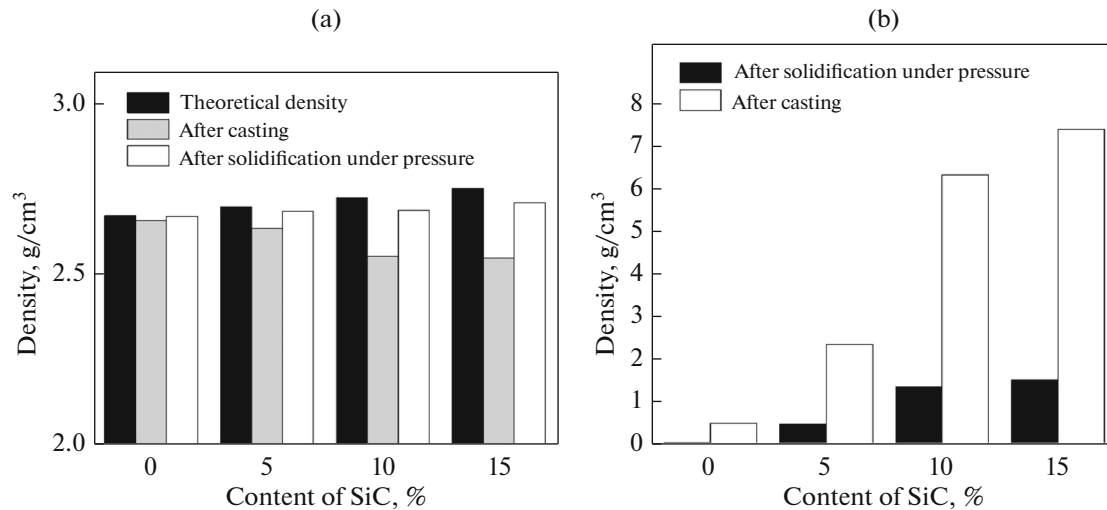


**Fig. 2.** Dependence of (a) the density and (b) the porosity on the content of the reinforcing particles in the composites in the cast state and after solidification under pressure.

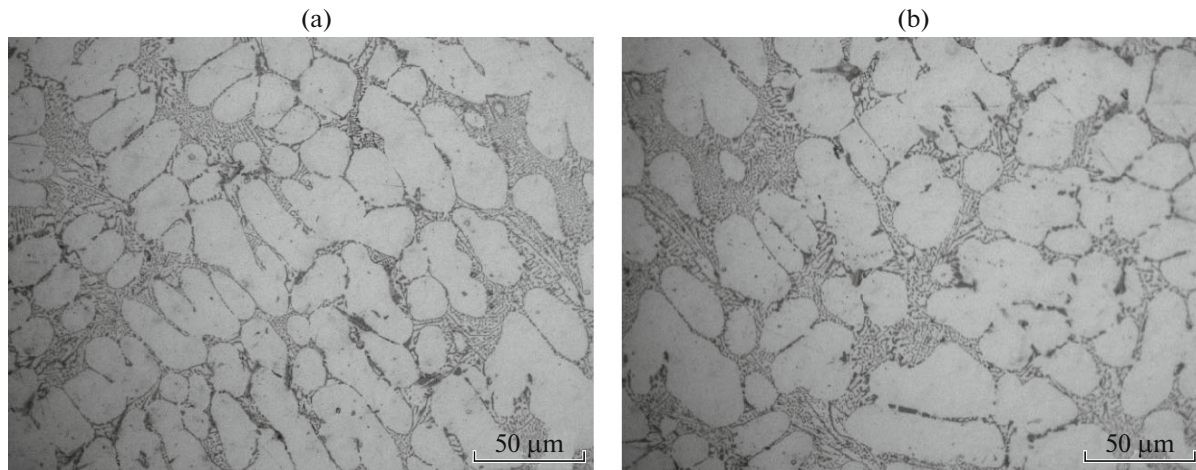


**Fig. 3.** Microstructure of the base alloy (a) in the cast state and (b) after solidification under pressure.

### 3.2. Study of the Microstructure of the Alloys

The microstructure of the base alloy in the cast state and after solidification under pressure is shown in Fig. 3. The structure of the base alloy mainly consists of an aluminum solid solution (Al) and a eutectic (Al)–(Si). Figure 4 shows the microstructure of composites with different contents of SiC particles. The quantitative analysis of the microstructure in the cast state (Figs. 4a, 4c, 4e) has shown that an increase in the quantity of SiC particles in the alloy leads to a decrease in the average size of dendritic cells. Thus, the average size of a dendritic cell for the base alloy was  $26 \pm 1.2 \mu\text{m}$ ; in the alloy with 5% SiC, it was  $22 \pm 1.1 \mu\text{m}$ ; at the content of 10% SiC, it was  $19 \pm 0.9 \mu\text{m}$ ; and, at the content of 15% SiC, the average size was  $18 \pm 0.7 \mu\text{m}$ . The decrease in the average size of den-

dritic cells can be explained by the action of SiC particles as barriers for the growth of dendrites in the process of solidification. In [16], it was shown that solidification under pressure leads to the formation of a finely dispersed structure due to the higher solidification rate. However, as can be seen from Table 1, the average size of dendritic cells hardly changes after solidification under pressure for all of the investigated alloys, which may indicate that the solidification rate changes insignificantly.

The microstructure of composites subjected to solidification under pressure is characterized by a more uniform distribution of particles and by a smaller porosity (Figs. 4b, 4d, 4f). As a rule, a uniform particle distribution inside the matrix leads to a reduction in the number of stress concentrators and to an improve-

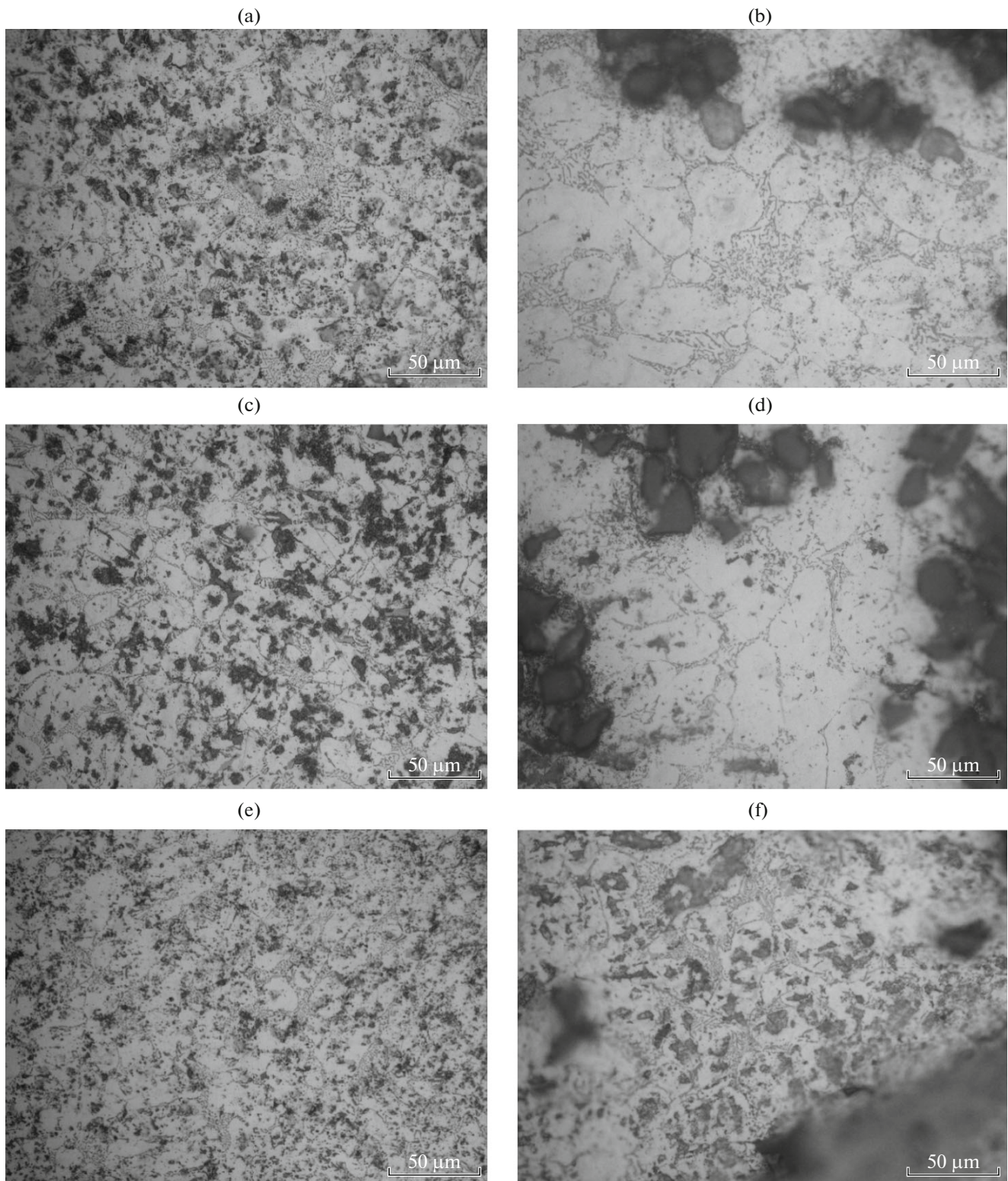


**Fig. 4.** Microstructure of composites in the cast state ((a) Al–9.1Si–0.58Mg/5% SiC; (c) Al–9.1Si–0.58Mg/10% SiC; (e) Al–9.1Si–0.58Mg/15% SiC) and after solidification under pressure ((b) Al–9.1Si–0.58Mg/5% SiC; (d) Al–9.1Si–0.58Mg/10% SiC; (f) Al–9.1Si–0.58Mg/15% SiC).

Average size of dendritic cells in the alloys in the cast state and after solidification under pressure

Material	Average size of a dendritic cell in the cast state, $\mu\text{m}$	Average size of a dendritic cell after solidification under pressure, $\mu\text{m}$
Al–9.1Si–0.58Mg	$26 \pm 1.2$	$25 \pm 0.9$
Al–9.1Si–0.58Mg + 5% SiC	$22 \pm 1.1$	$22 \pm 0.8$
Al–9.1Si–0.58Mg + 10% SiC	$19 \pm 0.9$	$19 \pm 1.0$
Al–9.1Si–0.58Mg + 15% SiC	$18 \pm 0.7$	$17 \pm 0.8$

ment of the mechanical properties. As was shown earlier [19], the application of high pressures in the process of solidification virtually excludes the appearance of shrinkage and gas porosities, interfacial micropores, and also ensures a good coupling at the interfaces between the particles and the matrix, which agrees with the results obtained in our work.

The influence of the process of the solidification of the composite with 15% SiC under pressure on its microstructure is demonstrated in Figs. 4e and 4f; it can be seen that there is a more uniform distribution of particles and a decrease in the amounts of agglomerates and pores. The analysis of the microstructure has shown that the nucleation of the primary aluminum solid solution occurs in the liquid between the particles rather than on the surface of the particles. This can be explained by a smaller thermal conductivity of SiC particles compared to the matrix alloy. The SiC particles cannot cool down so rapidly as the melt; as a result, the temperature of the particles proves to be higher than the temperature of the liquid alloy. Therefore, the process of solidification is retarded near the surface of the particles and the nucleation of the primary crystals of the aluminum solid solution occurs at a distance from the particles, where the temperature is lower [19, 20].

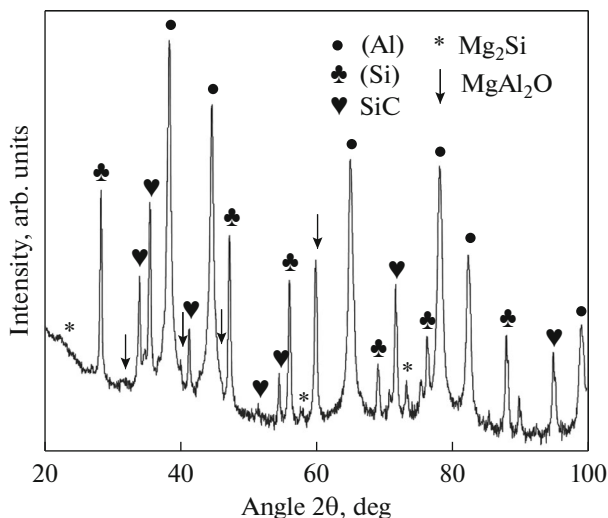


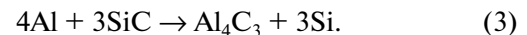
Fig. 5. XRD pattern of the Al–9.1Si–0.58Mg/15% SiC alloy after solidification under pressure.

### 3.3. Phase Composition of the Composites

As follows from the results of the X-ray diffraction analysis (Fig. 5), the structure of the composites subjected to solidification under pressure contains solid solutions (Al) and (Si) and compounds  $\text{Mg}_2\text{Si}$ ,  $\text{MgAl}_2\text{O}_4$ , and SiC. The presence of magnesium in the alloy not only leads to an improvement of mechanical properties, but also has a strong effect on the structure formation in the process of the mixing of particles into the melt and upon the subsequent solidification under pressure [2]:

—magnesium favors an increase in the wettability of SiC particles by the aluminum melt, which is especially important for the process of solidification under pressure;

—magnesium favors the formation of  $\text{MgAl}_2\text{O}_4$  or MgO on the surface of the oxidized SiC particles according to Eq. (2), which prevents SiC particles from interacting with Al according to Eq. (3) as follows:



The appearance of new phases in the interfaces as a result of the process of solidification under pressure can indicate an improvement in the wettability between the aluminum matrix and SiC particles, which leads to an increase in the coupling between them and, as a consequence, to an improvement of the mechanical properties. This agrees well with the results of other researchers [21–23] obtained earlier.

### 3.4. Hardness of Composites after Heat Treatment

Figure 6 displays a change in the hardness of the base alloy and composites obtained as a result of solidification under pressure, upon aging at a temperature of  $150^\circ\text{C}$ . Upon the aging, there are consecutively precipitated and dissolved coherent (Si/Mg clusters, Guinier–Preston (GP) zones) and semicoherent ( $\beta''$  phase,  $\beta'$  phase) particles, which leads to the presence in the aging curve of several local maxima [24–27]. As can be seen from Figs. 6 and 7, the values of the hardness in the composites are higher than in the base alloy both after quenching and in the maximum in the aging curve. This is related to the presence in their structure of SiC particles, the hardness of which is greater than

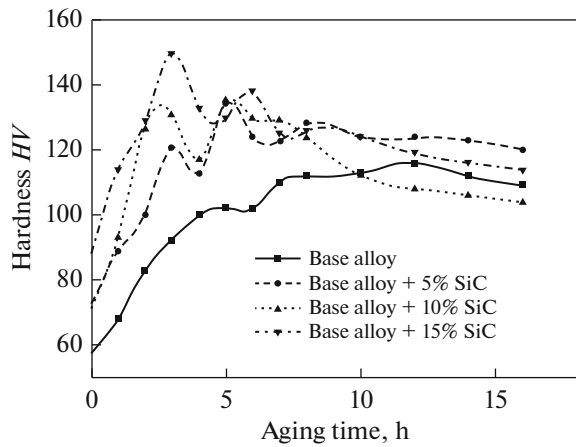


Fig. 6. Dependence of the hardness of composites on the time of aging at a temperature of 150°C.

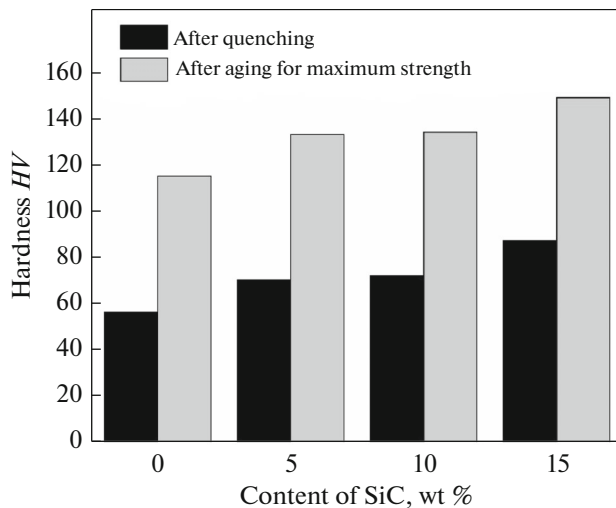


Fig. 7. Dependence of the hardness of composites after quenching and after aging for the maximum strength on the content of the reinforcing particles of SiC.

that of the aluminum solid solution, as well as to the strengthening of the matrix by dislocations that are generated near the particles in the process of solidification. In this case, the maximum value of the hardness is attained considerably more rapidly in the composites compared to the base alloy. This effect, which is connected with the presence in the materials with reinforcing particles of an enhanced dislocation density generated in the process of solidification, was also shown to take place in the Al–SiC/Al<sub>2</sub>O<sub>3</sub> composites [28]. However, because of the enhanced density of dislocations, more rapid softening occurs during the prolonged aging of composites. The most significant drop in the hardness after 16-h aging is observed in the composite with 15% SiC (by about 30 HV relative to the maximum value) and in the composite with 10%

SiC (by about 25 HV). The drop in the hardness of the base alloy was only 5 HV.

## CONCLUSIONS

(1) Composite materials based on the alloy of the Al–Si–Mg system reinforced by 5, 10, and 15 wt % SiC particles have been obtained by the method of introducing particles into the melt and by subsequent solidification under pressure.

(2) The microstructure of the composites after solidification under pressure is characterized by a smaller porosity and by a more uniform distribution of SiC particles as compared to the composites obtained by casting after the introduction of particles into the melt. As was shown by the XRD analysis, the application of a high pressure during solidification increases the wettability and the interaction between the particles and matrix at their interface.

(3) The introduction of particles into the structure of the matrix alloy leads to an acceleration of the aging process. The maximum in the kinetic curve of aging is achieved in 12 h for the base alloy and in 3 h for the composite containing 15 wt % SiC particles. The acceleration of the aging process is connected with a considerable increase in the dislocation density in the composites reinforced by particles.

## ACKNOWLEDGMENTS

The work was carried out at financial support from The Ministry of Education and Science of RF according to the Program of increasing Competitive Ability of The National University of Science and Technology MISiS among and in the row of leading world scientific-research centers in 2013–2014 within the framework of State Task no. 11.1760.2014/K.

## REFERENCES

1. M. T. El-Hair, “Microstructure characterization and tensile properties of squeeze-cast Al–Si–Mg alloys,” *Mater. Lett.* **59**, 894–900 (2005).
2. O. Beffort, S. Long, C. Cayron, J. Kuebler, and A. Buffat, “Alloying effects on microstructure and mechanical properties of high volume fraction SiC-particle reinforced Al–MMCs made by squeeze casting infiltration,” *Comp. Sci. Tech.* **67**, 737–745 (2007).
3. M. T. El-Hair, A. Lotfy, A. Daoud, and A. M. El-Sheih, “Microstructure, thermal behavior and mechanical properties of squeeze cast SiC, ZrO<sub>2</sub> or C reinforced ZA27 composites,” *Mater. Sci. Eng., A* **528**, 2353–2362 (2011).
4. A. Yu. Churyumov, A. I. Bazlov, A. N. Solonin, V. Yu. Zadorozhnyi, G. Q. Xie, S. Li, and D. V. Louzguine-Luzgin, “Structure and mechanical properties of Ni–Cu–Ti–Zr composite materials with amorphous phase,” *Phys. Met. Metallogr.* **114**, 773–778 (2013).
5. A. I. Bazlov, A. Yu. Churyumov, and A. A. Tsarkov, “Studies of the structure and mechanical properties of

- Ti<sub>43.2</sub>Zr<sub>7.8</sub>Cu<sub>40.8</sub>Ni<sub>7.2</sub>Co<sub>1</sub> alloy containing amorphous and crystalline phases,” *Phys. Met. Metallogr.* **116**, 684–689 (2015).
6. M. Aydin, R. Gürler, and M. Türker, “The diffusion welding of 7075Al–3% SiC particles reinforced composites,” *Phys. Met. Metallogr.* **107**, 206–210 (2009).
  7. V. I. Kuz'min, V. I. Lysak, S. V. Kuz'min, and V. O. Kharlamov, “Effect of heat treatment on the structure and properties of steel–aluminum composite with a diffusion barrier,” *Phys. Met. Metallogr.* **116**, 1096–1102 (2015).
  8. V. A. Popov and V. V. Cherdyn'tsev, “Formation of a nanodispersed metal–matrix structure during a combined high-energy mechanical alloying of powders of aluminum-based SiC-containing alloys,” *Phys. Met. Metallogr.* **107**, 45–52 (2009).
  9. A. V. Pozdniakov, A. Lotfy, A. Qadir, and V. S. Zolotarevskiy, Influence of B<sub>4</sub>C on the structure and coefficient of thermal expansion of the metal matrix composite material based alloy Al-5% Cu,” *Phys. Met. Metallogr.* **117**, (in press) 2016.
  10. G. Ranganath, S. C. Sharma, M. Krishna, and M. S. Muruli, “A study of mechanical properties and fractography of ZA-27/titanium-dioxide metal matrix composite,” *J. Mater. Eng. Perform.* **11**, 408–413 (2002).
  11. K. H. Seah, S. C. Sharma, and B. M. Grish, “Mechanical properties of as-cast and heat-treated ZA-27/graphite particulate composites,” *Comp. A: Appl. Sci. Manufac.* **28**, 251–256 (1997).
  12. X. Fan, X. Yin, X. Cao, L. Chen, L. Cheng, and L. Zhang, “Improvement of the mechanical and thermophysical properties of C/SiC composites fabricated by liquid silicon infiltration,” *Comp. Sci. Tech.* **115**, 21–27 (2015).
  13. P. K. Rohatgi, S. Alaraj, R. B. Thakkar, and A. Daoud, “Variation in fatigue properties of cast A359–SiC composites under total strain controlled conditions: Effects of porosity and inclusions,” *Comp. A: Appl. Sci. Manufac.* **38**, 1829–1841 (2007).
  14. M. Kok and K. Ozdin, “Wear resistance of aluminum alloy and its composites reinforced by Al<sub>2</sub>O<sub>3</sub> particles,” *J. Mater. Process. Technol.* **183**, 301–309 (2007).
  15. P. Poddar, V. C. Srivastava, P. K. De, and K. L. Sahoo, “Processing and mechanical properties of SiC reinforced cast magnesium matrix composites by stir casting process,” *Mater. Sci. Eng., A* **460–461**, 357–364 (2007).
  16. L. J. Yang, “The effect of solidification time in squeeze casting of aluminum and zinc alloys,” *J. Mater. Process Technol.* **192–193**, 114–120 (2007).
  17. M. Schöbel, W. Altendorfer, H. P. Degischer, S. Vaucher, T. Buslaps, M. Michiel, and M. Hofmann, “Internal stresses and voids in SiC particle reinforced aluminum composites for heat sink applications,” *Comp. Sci. Technol.* **71**, 724–733 (2011).
  18. R. S. M. Seyed, “Processing of squeeze cast Al6061–30 vol % SiC composites and their characterization,” *Mater. Design* **27**, 216–222 (2006).
  19. M. T. El-Khair, “Microstructure characterization and tensile properties of squeeze-cast AlSiMg alloys,” *Mater. Lett.* **59**, 894–900 (2005).
  20. A. Daoud, “Microstructure and tensile properties of 2014 Al alloy reinforced with continuous carbon fibers manufactured by gas pressure infiltration,” *Mater. Sci. Eng., A* **391**, 114–120 (2005).
  21. M. Kok, “Production and mechanical properties of Al<sub>2</sub>O<sub>3</sub> particle reinforced 2024 aluminum alloy composites,” *J. Mater. Process. Technol.* **161**, 381–387 (2005).
  22. H. Young and G. Chung, “The effect of applied pressure on particle–Dispersion characteristics and mechanical properties in melt-stirring squeeze cast SiC/Al composites,” *J. Mater. Process. Technol.* **55**, 370–379 (1995).
  23. B. Li, B. Luo, K. He, L. Zeng, W. Fan, and Z. Bai, “Effect of aging on interface characteristics of Al–Mg–Si/SiC composites,” *J. Alloys Compd.* **649**, 495–499 (2015).
  24. H. Liao, Y. Wu, and K. Ding, “Hardening response and precipitation behavior of Al–7% Si–0.3% Mg alloy in a pre-aging process,” *Mater. Sci. Eng., A* **560**, 811–816 (2013).
  25. R. Dong, W. Yang, Z. Yu, P. Wu, M. Hussain, L. Jiang, and G. Wu, “Aging behavior of 6061Al matrix composite reinforced with high content SiC nanowires,” *J. Alloys Compd.* **649**, 1037–1042 (2015).
  26. J. Banhart, C. S. T. Chang, Z. Q. Liang, N. Wanderka, M. D. H. Lay, and A. J. Hill, “Natural aging in Al–Mg–Si alloys—A process of unexpected complexity,” *Adv. Eng. Mater.* **12**, 559–571 (2010).
  27. M. R. Gazizov, A. V. Dubina, D. A. Zhemchuzhnikova, and R. O. Kaibyshev, “Effect of equal-channel angular pressing and aging on the microstructure and mechanical properties of an Al–Cu–Mg–Si alloy,” *Phys. Met. Metallogr.* **116**, 718–729 (2015).
  28. I. Dutta, S. M. Allen, and J. L. Hafley, “Effect of reinforcement on the aging response of cast 6061–Al<sub>2</sub>O<sub>3</sub> particulate composite,” *Metall. Trans. A* **22**, 2553–2563 (1992).

*Translated by S. Gorin*